RC24724 (W0901-047) January 13, 2009
Electrical Engineering

IBM Research Report

Experimental and Theoretical Explanation for the Orientation Dependence Gate-Induced Drain Leakage in Scaled MOSFETs

P. M. Solomon, S. E. Laux, L. Shi, J. Cai, W. Haensch
IBM Research Division
Thomas J. Watson Research Center
P.O. Box 218
Yorktown Heights, NY 10598

Research Division
Almaden - Austin - Beijing - Cambridge - Haifa - India - T. J. Watson - Tokyo - Zurich

Experimental and theoretical explanation for the orientation dependence gate-induced drain leakage in scaled MOSFETs.

P. M. Solomon, S.E. Laux, L. Shi, J. Cai and W. Haensch
IBM, SRDC, T.J. Watson Research. Center, Yorktown Heights, NY 10598, e-mail: solomonp@us.ibm.com
Tel: (914) 945-2841, Fax: (914) 945-2141, Email: solomonp@us.ibm.com

ABSTRACT

In this work we provide a compelling experimental and theoretical explanation for the low GIDL currents that occur due to band to band (b2b) tunneling in MOSFETs with <100> (45º rotated) channel direction compared to <110> oriented devices. In measurements on bulk Si wafers, we clearly show a factor of ~3x decrease in tunneling current for (001) wafers compared to (011) or (111) orientations supporting the GIDL observations. Rigorous calculations of complex band structure for the three directions reveal that the light hole band dominates the tunneling action integral, supporting our measurements and accounting for the GIDL data.

INTRODUCTION

As technology is scaled down, b2b tunneling becomes an increasingly important source of leakage [1] as is manifested in GIDL currents. GIDL shows an unexplained dependence of the orientation of a FET in the plane of the (100) silicon wafer. When the FET is aligned with the flat [110] direction) the GIDL are significantly higher than when aligned at 45º (100 direction), as shown in Fig. 1. As a result ultra-low leakage FETs are commonly aligned at 45º. In contradiction to this, standard b2b models [2,3] predict the 100 direction to be the easy tunneling direction (highest current) mainly because the four Si conduction-band valleys have a light electron-mass in this direction compared with only two such valleys in the 110 direction. To resolve this discrepancy we measure, systematically for the first time, tunneling currents in planar p-n junction diodes on wafers oriented in [001], [110] and [111] directions, and also generate an accurate complex silicon band structure in each of these directions. Tunneling action integrals are calculated directly from the complex bands rather than relying the poor approximation of band edge masses. Our experimental and theoretical results provide a consistent and conclusive explanation for the orientation dependence of GIDL in MOSFETs.

EXPEROMENTAL METHODOLOGY

We follow the experimental methodology of [4] with the difference that a heavily doped buried layer is used in place of a heavily doped substrate. Small samples are used (5 and 10 μm dia.) to reduce the impact of series resistance. The N-on-P LOCOS isolated diodes were fabricated on [001], [011] and [111] substrates on four quadrants of two wafers. TSUPREM simulations are shown in Fig.2 indicating implant conditions. IV was measured with the HP 4142B SMU unit and CV was measured with the HP 4294A LCR meter, at 1MHz. Following ref 3, doping profiles were derived from the CV curves by assuming an exponential doping profile ($N(x) = N_{b0} - \exp(x/\lambda)$) where N_{b0}, λ and the bandgap are the adjustable parameters. Once the profile has been derived the effective tunnel distance [4] can be calculated for any applied voltage.

THEORY

Complex bands were computed for Si in three directions: [100], [110] and [111], based on an atomistic $sp^3d^5s^*$ Hamiltonian with spin-orbit coupling. The complex band computation follows Boykin[5,6] modified for nearest neighbor coupling only.

RESULTS AND DISCUSSION

IV characteristics of diodes for the three orientations and two B doping conditions (Q2 and Q5 in Fig. 2) are shown in Fig. 3a, and CV measurements for conditions Q2, Q3 and Q5 are shown in Fig. 3b. Note the strong enhancement of tunneling current for the 011 and 111 wafers. This cannot be explained by profile differences as derived from the CV measurements. An example of such a doping profile is shown in Fig. 4. While the profile obviously has a lot of noise and uncertainty, the tunnel distance calculated from the profile is relatively insensitive to the profile parameters (see Fig. 5) provided the capacitance at low voltages is accurately determined. Current density vs. effective tunneling distance[4] is shown in Fig. 6., where segments of the curves are at constant voltages, each point from a separate quadrant. Note how strikingly the data are unified, as in ref. 3, but now including both the [011] and [111] directions, which show higher currents than 001 in agreement with GIDL observations. The effective mass and prefactor (averaged over all segments) was derived from the slope and intercept of each segment as show in Table 3.

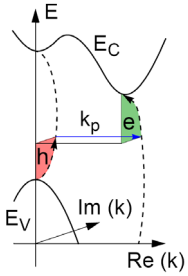

Turning to theory; the complex band structure of silicon was calculated for the three directions. As shown schematically in the figure opposite, the integral is started along the hole branch, shifted by a suitable phonon wave vector, k_p, to the electron branch, and then continued to the conduction band minimum. For clarity, in Fig. 7, the E-Im k plane only is shown, resulting in a juxtaposition of the electron and hole branches. The action integral $\int k.dx = \int k.dE / eF$, where F is an assumed constant field and we call $\int k.dE$ the energy action integral. In Fig. 7 the energy action integrals are the shaded areas divided into electron and hole components. Their values, indicated in the figure for the three orientations, show a strong correlation with the experimental trends. The slope, S, of log[current] vs tunneling distance is related to this integral by $S = 2\int k.dE/E_G$. Slopes corresponding to the Fig. 7 numbers are superimposed on Fig. 6 (dotted and dot-dashed lines), where the agreement is quite striking. (This somewhat contradicts the data derived from the slopes of the segments, in Table 1, but this is within experimental error).

CONCLUSIONS

We have explained the reduction of GIDL in [001] compared to [011] directions and furthermore have shown that the [001] direction is the hardest b2b tunneling direction compared to both [011] and [111] directions. Our calculations of complex band structure of Si for these directions, and the tunneling energy-action integrals, show strong correlation with the experimental results and offer an explanation whereby the light hole-band dominates the action integral.

1. P. Gilbert, A. Steegen et.al, IEDM 2007, dig. p. 259.
2. Fischetti, O'Regan *et al*, IEEE Trans. Electron. Dev, 54, 2116, (2007).
3. A. Schenk, Sol. State Electron., **36**, 19 (1993).
4. P.M. Solomon, D.J. Frank, *et al*., J. Appl. Phys., **95**, 5800 (2004).
5. T.B. Boykin, Phys Rev. B, **54**, 8107 (1996).
6. T.B. Boykin and G. Klimeck, Phys Rev. B **71**, 115215 (2005).

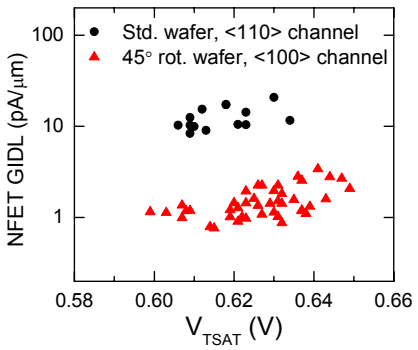

Fig. 1: Measured NFET GIDL dependence on substrate type in CMOS 65nm low power technology [1].

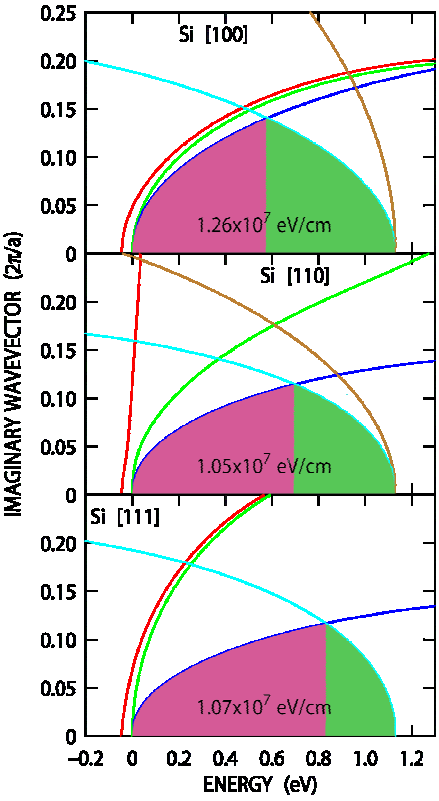

Fig. 7: Imaginary band structure for the principle directions in Si. The shaded area is the energy action integral, $\int k.dE$, with the hole and electron components colored maroon and green respectively.

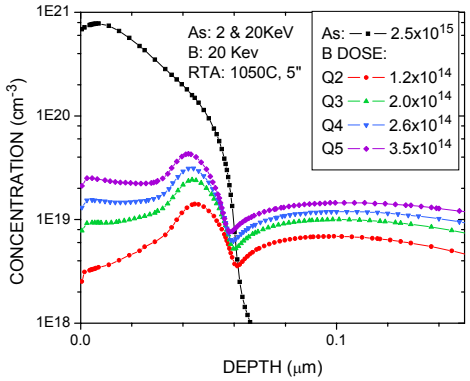

Fig. 2: TSUPREM simulations of ion implantation and rapid thermal anneals.

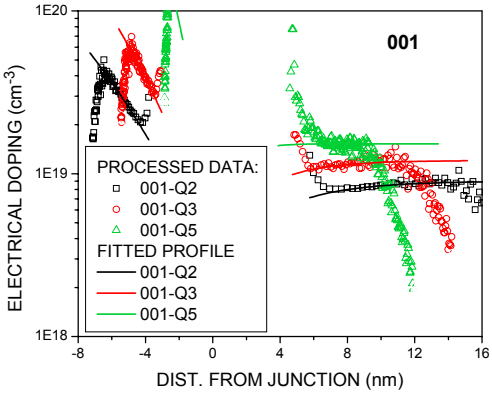

Fig. 4: Doping densities calculated from CV data, compared to the fitted exponential profiles for a 001 wafer.

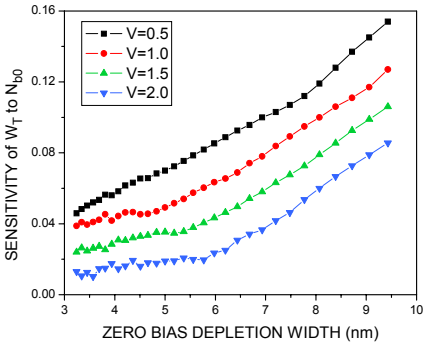

Fig. 5: Relative sensitivity of effective tunneling distance to changes in N_{b0} at a constant zero-bias depletion width.

Fig6: Tunneling current density at a constant applied voltage vs. effective tunneling distance for 001, 011 and 111 tunneling directions. The dashed lines are at slopes corresponding to actions integrals of 1.05 and 1,25 eV/nm assuming a bandgap of 1.05eV.

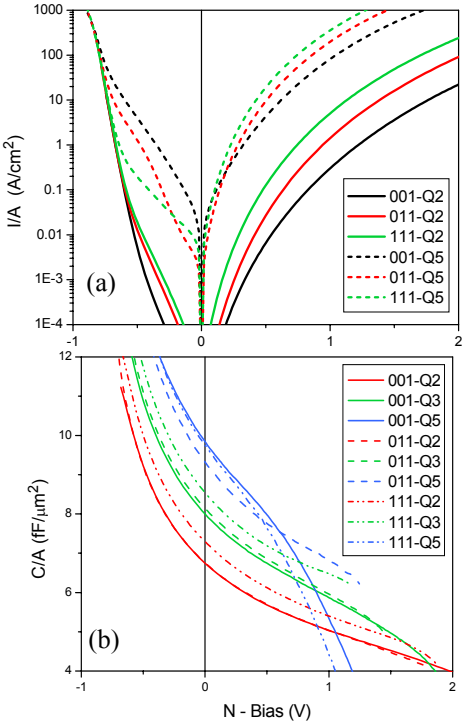

Fig. 3: (a) Current density vs voltage for Q2 and Q5 for all crystal orientations. (b) CV curves, at 1MHz, for Q2, Q3 and Q5 for all crystal orientations. Downturn in curves at high bias is caused by

Orien.	m_T	J_{T0} @ ***0.8V*** (A/cm^2)	J_{T0} @ ***1.6V*** (A/cm^2)
001	0.21	2.2e6	1.4e7
011	0.21	1.9e7	3.8e7
111	0.21	2.1e7	3.8e7

Table 1: Effective mass (averaged over voltage segments) and current density prefactor at two applied voltages, for the 001, 011 and 111 tunneling directions, based on the data of Fig. 6.